A Swallowable diagnostic capsule with a direct access sensor using anisotropic conductive adhesive

Pio Jesudoss, Alan Mathewson, Karen Twomey and Frank Stam

Heterogeneous System Integration Group, Microelectronics Applications Integration

Tyndall National Institute

Cork, Ireland

+353214904441, pio.jesudoss@tyndall.ie

William M.D. Wright

Department of Electrical and Electronic Engineering

University College Cork

Cork, Ireland

***Abstract*— Technological developments in biomedical microsystems are opening up new opportunities to improve healthcare procedures. Swallowable diagnostic sensing capsules are an example of this. In this paper, a novel direct access sensor (DAS) has been demonstrated which uses Flip Chip (FC) technology to expose the sensor to the liquid medium. An electrochemical study showed that the Anisotropic Conductive Adhesive (ACA) joint provides good connection and does not impair the sensor functionality. The reliability test results showed that most of the samples survived the humidity aging test and that only 2 out of 9 ACA connections of the same electrode failed. For the failed samples, the failure analysis showed that the tensile stress at the chip/epoxy interface caused a delamination at this interface.**

Keywords-component; Anisotropic conuctive ahesive (ACA); Flip hip Over Hole (FCOH); Direct Access Sensor (DAS); reliability; swallowable diagnostic sensing capsule.

I. INTRODUCTION

In medicine, Inflammatory Bowel Disease (IBD) is a group of inflammatory conditions that affect the Gastro-Intestinal (GI) tract [1]. Although the IBD can be divided into several categories, the two major forms of IBD are Crohn's disease (CD) and ulcerative colitis (UC) [2]. There has been a rapid growth of IBD in Europe and North America during the second half of the twentieth century and it is becoming more prevalent in the rest of the world as they adopt the western life style [3]. CD and UC are chronic disease which can lead to long-term and sometime irreversible impairment of the GI tract [1].

One of the conventional methods to investigate any suspected pathology is to use an endoscope which is inserted through patient's mouth, nose or rectum. These procedures provide some information: gastroscopy provides information about the Oesophagus and the stomach while the colonoscopy helps investigate the large intestine. These procedures are not only unpleasant for the patients but are also unable to provide information from the small intestine.

With recent advances in microelectronics, wireless communication and sensor development, the limitations of endoscopy is overcome in the format of a biomedical swallowable capsule [4]. The swallowable capsule is an autonomous system which contains a sensor, the associated electronics for signal conditioning and amplifying and a radio transmitter all encapsulated in a biocompatible material. The swallowable capsule involves a non-invasive technique which can provide information about the whole GI tract. The concept of first radio telemetry ingestible capsule was put forward by R.Stuart Mackay and Bertil Jacobson in 1957 [4, 5].The swallowable capsules can be classified into families of imaging (PillCam, Olympus Optical) [5-7], drug delivery systems [5, 7, 8] and sensing capsules [4, 5, 7-15]. Unlike the imaging and the drug delivery capsules where none of the parts are exposed, the chemical sensing capsules have one or more sensors that measures biochemical variables related to the gut ecosystem through exposed sensors. But in none of the diagnostic sensing capsules, the sensor attachment -the first level packaging of the

sensor in a swallowable capsule- is achieved by Flip Chip Over Hole (FCOH) method using anisotropic conductive adhesive. ACA's relatively simple process steps [16] make it suitable for bonding a DAS. In a DAS, ACA not only provides the electrical interconnection but simultaneously seals the interconnect area and the underlying electronics from the sensor area in a capsule application, as shown in Fig. 1. The adhesive is more prone to moisture uptake than chip or metals used in track and pads [17]. The capsule transition through the GI tract takes around 72hrs during which the epoxy matrix will come in direct contact with GI fluids. As the adhesive comes in contact with fluid, one of the most severe tests to be considered is the moisture sensitivity test. As there are no standardarized test procedures that could be found for biomedical humidity aging, the moisture humidity test was considered at 50˚C/95%RH to study the reliability of the ACA for a DAS.

This paper describes the DAS achieved through FCOH and its endurance in terms of reliability of the ACA joint during humidity aging. The following section describes the development of the DAS and its electrochemical testing. This was followed by the reliability study of the DAS ACA joint and conclusion.

II. DAS DEVELOPMENT AND ELECTROCHEMICAL TEST

A. *Chip*

The test chip is a 6x6mm^2 die with a thickness of 0.525mm. It was fabricated using a multi-layer silicon technology and photolithography techniques. Gold and platinum were deposited on the chip sensing area. The sensing chip has 5 pads on the periphery with Input/Output (I/O) pad size of 300 micron square as shown in Fig. 2(a).The microelectronic sensor comprised of four gold working electrodes (WE) of 1 mm diameter and a platinum counter electrode (CE) of 2mm diameter. The distance between centers of counter electrode and the working electrode was set at 0.5mm. The sensor chip electrodes are used to evaluate the liquid medium with cyclic voltammetry.

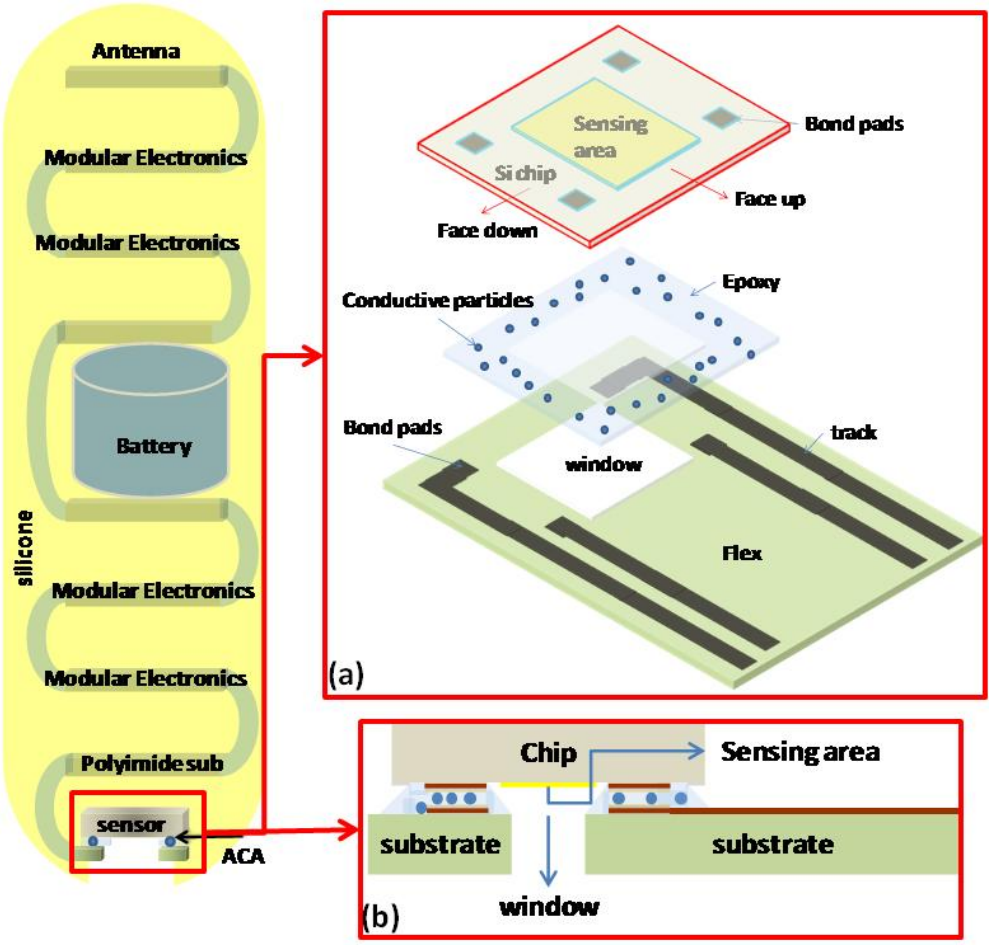

Fig. 1 Schematic of capsule with expanded image of FCOH (a) and (b) Cross sectional view of FCOC/DAS interconnections based on ACA

B. Test Substrate

A single layer thin polyimide substrate with thickness 0.025mm was fabricated. The copper track on the flexible substrate was 15µm thick while on the bond pads an additional 5µm Ni and 0.05µm of electroplated flash gold was deposited. The flexible substrate is 77mm long, with a circular part of radius 6 mm at one end, a 3mm wide middle section and a 11.25mm width fanned out region on the other end. A square window of 4.4mm was cut from the centre of the board with a laser cutting tool to expose the sensors to the external environment, see Fig. 2(b).

C. Assembly process

A pre-cleaning procedure was carried out separately on both the chip and the substrate. This involved placing the chips and the substrates into a barrel type chamber of a March Plasmod system and exposing them to an oxygen plasma for 40sec at 150 watts. This was followed by IPA immersion in a bench top ultraware ultrasonic precision cleaner for 5 minutes followed by a DI water rinse. The samples were then dried in a conventional Heraeus vacuum oven at 150˚C for an hour.

Gold stud bumps were formed on the die pads using a Kulicke and Soffa ball wedge gold bonder. The bumps had a mean diameter of 103µm and a mean height of 108µm. The gold stud bump was coined at 26N/mm^2 at a coining temperature of 180ºC for 20 sec and the coined bump's diameter and the height were around 123µm and 18µm respectively.

ACA material from Loctite was dispensed on the test board using a CAM/ALOT 1414 liquid dispense system. A brown viscous epoxy paste with gold coated nickel filler particles of 7µm was used. The alignment and bonding of the chip/substrate was performed using Finetech Flip-Chip bonder. Bonding was carried out at a ramp rate of 2K/sec with a hold at 180°C for 40 sec and a cool down rate at 3K/sec and with a bonding pressure of 22N/mm^2 for 8 sec. The average bond line thickness of the adhesive taken from 10 samples was approximately 21µm with a standard deviation of 1µm.

D. DAS packaging

The test assemblies were then encapsulated in silicone. The encapsulation process consisted of the following: A region of silicone was dispensed on the perimeter of the window using

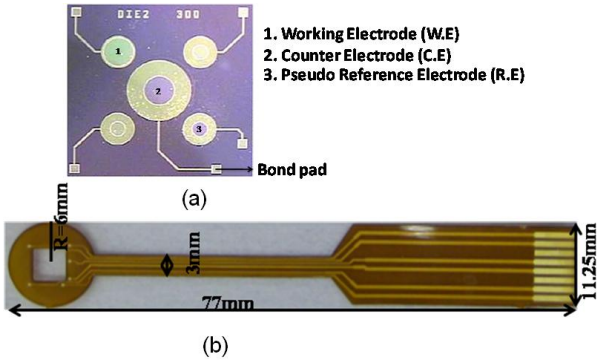

Fig. 2. (a) The direct access sensor chip and (b) Flexible substrate with window opening for sensor access.

CAM/A LOT and cured in the oven at 80°C for 3hrs. The cured silicone acted as a dam around the window. The protection of the sensor was achieved by applying AZ photoresist – Diazonnaphthoquinones (AZ Electronic Materials GmbH) via pendant drop method - 6 drops of AZ on the sensor area - and cured at 80°C for 1 hr. This had a height of around 596.7µm and acted as a plug covering the exposed area of 19.36mm^2. Once the dam and the plug were ready, the assembly was inserted into a gelatin glycerin capsule (33mm*13mm) and secured in place. The fixed assembly was then filled with silicone and cured at room temperature for 24 hrs. This was followed by immersing the capsule in warm water (50°C) for 10-15 minutes to dissolve the glycerin capsule. The sensor was then exposed by dissolving the AZ photoresist in acetone for 5-10 minutes, as shown in Fig. 3.

E. DAS Testing – Cyclic Voltammetry

The electrical connection and the robustness of the packaging as well as the functionality of the sensor were tested using cyclic voltammetry on the three electrode cell comprising of WE, CE and the Pt R.E on the sensing chip. In such an analytical electrochemical setup CE, WE and R.E are placed in an electrolyte, the current is passed between the WE and the CE and the voltage measurement is made between WE and the R.E. Elecrochemical reactions occurring at the interface between the WE and the solution were monitored by a CH instruments 620B computer controlled potentiostat. The fabricated test assemblies were dipped into a solution of 0.5M of H_2SO_4 and cyclic voltammetry test at a scan rate of 0.2V/sec was applied to the electrode system. The chemical reactions that occurred at the gold WE in this solution are well documented [18] and any change in the performance of ACA or the component will be identified at this stage.

F. Results of DAS Testing – Cyclic Voltammetry

Fig. 4 shows the plot of current versus potential for a forward and reverse sweep as a result of the cyclic voltammetry. A peak was obtained at 1.4V during the positive voltage sweep – oxidation (ox) - from 0 to 1.5V, and a corresponding peak was obtained at 0.9V during the negative voltage sweep, reduction (red). These gold peaks were due to gold oxide formation and reduction and the corresponding gold reactions taking place are shown in equation (1) [19], and they illustrated the correct function of the sensor and interconnect.

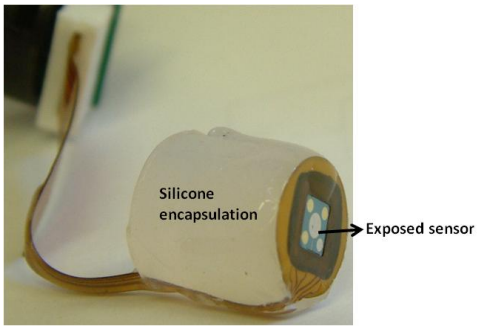

Fig. 3. Package sensor.

$$2Au + 3H_2O \rightarrow Au_2O_3\,(hyd) + 6H^+ + 6e^- \quad (ox)$$
$$Au_2O_3\,(hyd) + H_2O \rightarrow 2AuO_2 + 2H^+ + 2e^- \quad (red) \qquad (1)$$

III. Reliability of the DAS ACA joint - Constant Humidity Aging

Once again, it is important to highlight that the ACA interconnect used in the DAS was destined to be used in the gut environment. It is crucial that the adhesive survive the 72 hour transition through the GI environment. As the adhesive comes in contact with fluid, one of the most severe tests that could be considered was the moisture sensitive test. As no standard test procedures that could be found for biomedical humidity aging, the constant humidity aging was carried out at 50˚C/95%RH to study the reliability of the ACA for a DAS. This part of the work focused on the endurance of the ACA attachment for a DAS.

A. Further Encapsulation process

Wires were soldered on to each flex board connector bond pads. A two part Polypropylene mould of 95mm length, 13.25mm wide and 0.3mm thick was fabricated where the first part had a base while the second part side was hollow. As shown in the cross-sectional Fig. 5(a), the sensor encapsulated sample was sandwiched between the base and the hollow mould and the edges sealed with glue. Silicone was poured and cured for 24 hrs. The cured sample was taken out by pulling the moulds apart and the encapsulated sample is shown in Fig. 5(b).

B. Electrical Measuremnts

As seen in Fig. 2(a), each electrode had its corresponding bond pad on the chip periphery. These bond pads made connection via the ACA joint to the matching band pad on the substrate thus making individual joint connection for each electrode. The DAS structure developed in this research was destined to be tested via electrochemistry and therefore an online four point measurement of the contact resistance was not possible. As a result the contact resistance of the ACA interconnect was measured using a HP 3441A multimeter

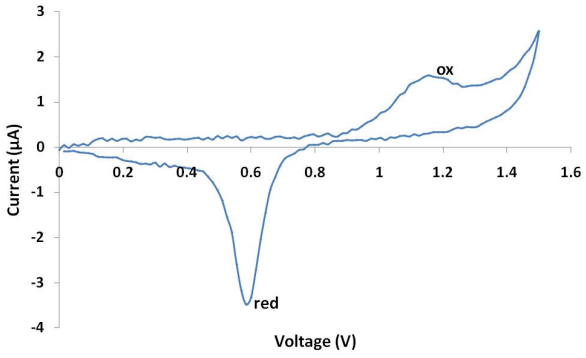

Fig. 4. Cyclic current-voltage curve of the Au W.E.

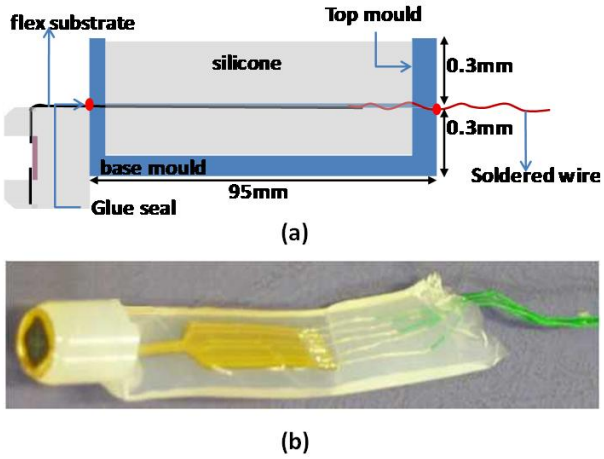

Fig. 5. (a) Cross-sectional schematic of the second encapsulation process and (b) picture of encapsulated sample for reliability testing.

acting as a two probe ohmmeter. The resolution of the resistance measurement is 1mΩ. The error in the repeatability of the measurement was in the order of 8-10mΩ. The measurement was made by placing the probe tip on the electrode surface and at the tip of the wire. The resistance was separately measured for the chip, and the substrate. The same measurements were conducted on the device – chip mounted on the substrate via ACA and encapsulated in silicone. The measurements carried out on the substrate and the chip were subtracted from the contact resistance measurement on the device, consequently measuring the contact resistance of the ACA joint.

C. Results and Discussion

A batch of 9 samples were made. Each sample had 5 sensor connections. Fig. 6 shows the variation of the adhesive joint contact resistance on the 5 different connections on the same sample versus the duration of hygrothermal aging at 50˚C/95%RH. It can be seen that the initial contact resistance of the 5 adhesive connections range from 100mΩ to 600mΩ. This discrepancy in the contact resistance could be explained by the number of conductive particles trapped in parallel configuration as shown in Fig. 7.

Fig. 8 shows the variation of ACA contact resistance corresponding to the same electrode connection of all 9 samples. Only 2 out of 9 ACA connections showed a slow increase in contact resistance until an open circuit was formed. It also showed that most of the samples showed no resistance drift during the whole reliability test. It can be seen in Fig. 6 and 8 that as the test went on, the contact resistance measurements showed some ripples that occurred at around 100 hrs of constant humidity aging.

As shown in Fig. 2 (a) only three electrodes noted 1, 2 and 3 were used in the electrochemistry. Only 2 out of 9 samples showed failure after hygrothermal aging for the contact joints representing the three electrodes. The samples that showed contact joint failure were samples 3 and 4. A 100% failure was observed in samples 3 and 4 at around 100hr of aging.

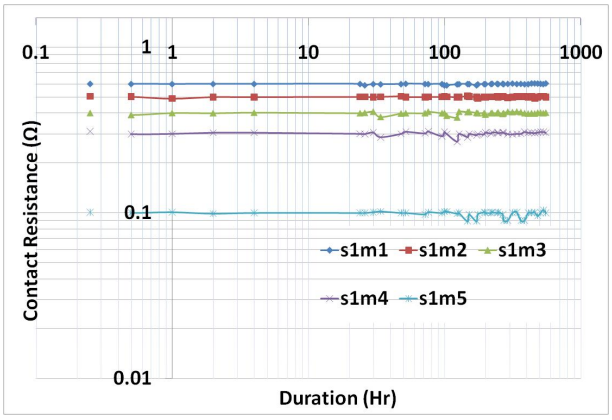

Fig. 6. Plot of ACA contact resistance vs. duration of humidity aging of all the electrodes in one sample.

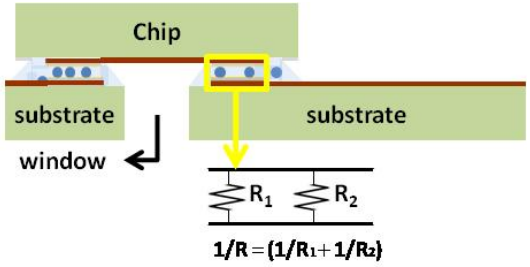

Fig. 7. Schematic of ACA interconnect showing the parallel configuration of the trapped conductive particles.

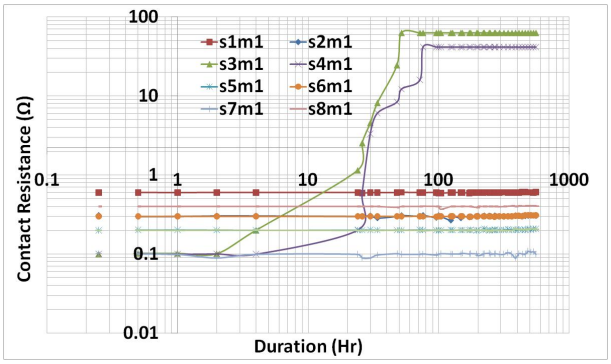

Fig. 8. Plot of ACA contact resistance vs. duration of humidity aging corresponding to the same electrode in all the 9 samples.

Epoxy expands due to moisture ingress while the silicon die and the other metal pads experience no expansion [20]. The loading conditions created a coefficient of thermal expansion (CTE) and coefficient of moisture expansion (CME) mismatch between the chip, substrate and the adhesive. Typical material parameters are shown in table 1.

Both CTE and CME mismatch between materials lead to thermal stress and hygroscopic stress at the interface between epoxy/chip and epoxy/flex substrate system. The diffusion coefficient is greater for the adhesive. This will force the adhesive to absorb more water than other materials in the humidity chamber. Moreover the CME of the adhesive is higher than other materials. In our package configuration, the epoxy swelling due to moisture absorption produced a perpendicular as well as parallel expansion of the epoxy with respect to the die and the substrate and induced tensile and shear stress at the ACF interface. However former studies have showed that when the epoxy is saturated with moisture, the swelling was uniform and that the induced shear stress was insignificant when compared to the normal stress [17, 20].

For contact resistance measurement the samples were taken out of the humidity chamber through a side door and the measurements were carried out manually at room temperature using HP 3441A multimeter. The samples were out of the chamber for around 5- 10 minutes. One previous study suggested that the momentary transfer of the sample in and out of the humidity chamber caused a temporary concentration gradient which lead to either absorption or desorption of water from the adhesive. This constant absorption and desorption would cause the materials to expand and shrink. This constant movement of the sample in and out of the chamber for testing could have caused microscopic sliding. This slow fatigue like process coupled with slow relaxation of the contact pressure could lead to a steady increase in contact resistance until an open circuit was observed [21]. This could explain the observed slow and steady degradation of the contact resistance shown in Fig. 8. The ripples that are observed could be attributed to the error in contact pressure when placing the probes on the sample during the measurement.

Polymer expansion due to moisture ingress and the mismatch of moisture expansion coefficients of materials may cause the formation of defects like cracks and delaminations [22, 23]. It is more likely that there are some initial microscopical delaminations present at the ACA interface caused by the defects present on the chip or substrate surface or by the process [20]. Moisture has an adverse effect on ACA's interfacial adhesion and may accelerate the delamination process by weakening the polymer interface. Fig. 10 (a) and (b) and Fig. 11 (a) and (b) present examples of the Scanning Acoustic Microscopy (SAM) study that was used to assess the sealing efficacy of the DAS before and after humidity testing. Fig.10 (a) and (b) show the SAM images of one the samples that survived the hygrothermal testing. No delamination was observed in the sample before and after humidity aging. On the contrary, Fig. 11 (a) and (b) show the SAM images taken on the failed samples after hygrothermal aging. It can be seen that

Table.1. Material parameters. Collected from [17, 24-26].

	Silicon chip	Polyimide substrate	Gold bump	ACA
Coefficient of thermal expansion (CTE) (ppm/ºC)	2.7	20	12.9	47
Coefficient of moisture expansion (CME) (mm^3/g) ($*10^2$)	0	1	0	4
Diffusion Coefficient (mm^2/s) ($*10^{-6}$)	$1e^{-24}$	5.0	$1e^{-24}$	9.7
Specific Heat, c (J/Kg-K)	700	1090	800	1000

there are delaminations present, these are indicated by rectangles on the figure, after the humidity aging. The moisture aging has a deleterious effect on the adhesion strength and the weakening of the adhesion is reflected by white patches in the SAM image. The SAM analysis does not show where the failure occurred and in order to get a precise picture of the failure a cross-sectional analysis was performed.

An Olympus BH2-UMA Optical microscope image of the samples that failed during aging were cross-sectioned and presented in Fig. 12. Failure occurred by an interfacial delamination at the epoxy/silicon and epoxy/bump interfaces. Previous studies have shown that the ACA adherence to another polymeric material is higher than that for silicon [27, 28]. In addition, the bump/pad interface was found open, resulting in the loss of conductivity and increase in resistance. The delamination seems to proceed along the chip passivation layer with a higher gap on the left side of the bump/pad towards the edge of the chip than on the right side of the bump/pad. This could imply that the delamination was initiated at the edge of the die. The disruption of the hydrogen bonds by water molecules caused plasticization in the short term by spreading the polymer molecules apart and causing expansion of the adhesive joint [29, 30]. In addition, the temperature gave rise to CTE mismatch between the adhesive and the other metals and contributed to the degradation of the ACA interface. Thus the interface was under tensile and shear stress with a

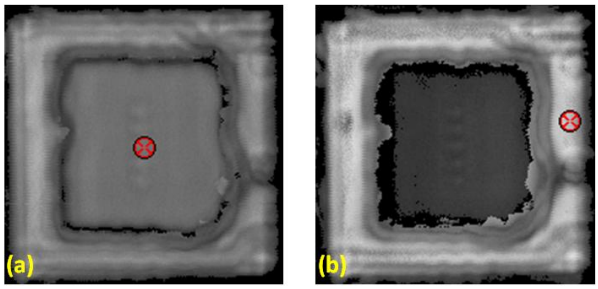

Fig. 10. SAM images (a) before and (b) after hygrothermal testing of one the samples that survived.

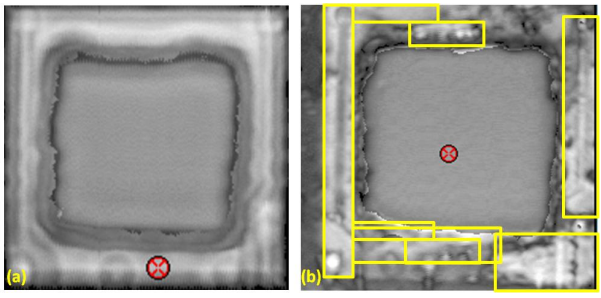

Fig. 11. SAM images (a) before and (b) after hygrothermal testing of one the samples that failed.

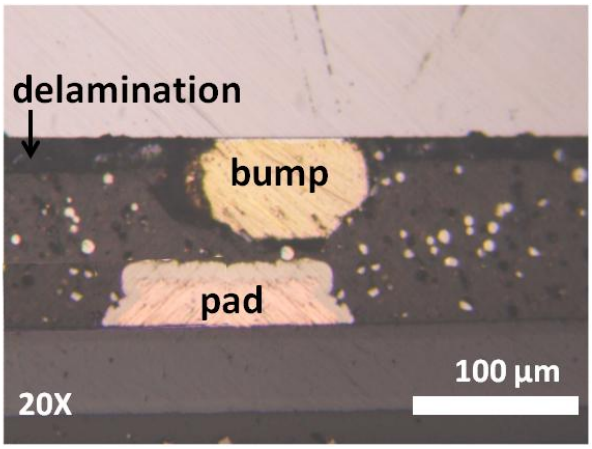

Fig. 12. Cross-section of samples after humidity testing - failure by crack propagation.

dominant tensile stress at the bump and die/epoxy interface. The fact that the delamination was parallel to the chip interface suggests that a pure tensile force was in action during the swelling process.

IV. Conclusion

In this study, a novel DAS has been developed with a modified FC technique to expose the sensor to the liquid medium. Furthermore ACA can be used as a suitable material for applications with few relatively large bond pads and particularly in relation to measurements in the fluidic environment when the sensing area needs to be sealed off from the electronics.

The electrochemical study of the ACA joint and the sensor after encapsulation with silicone showed the ACA joint provides good connection and the electronic functionality and chemical sensing performance wasn't compromised.

The reliability of the ACA attachment for a DAS was studied by constant humidity aging. At the end of the reliability test, out of the 9 samples tested, for the same electrode in all 9 samples, only 2 of the ACA connections exhibited a slow increase in resistance until an open circuit was observed. The slow resistance increase of the failed joint was attributed to a fatigue like process induced by removal and replacement of the sample in the humidity chamber. Failure analysis of the failed joint after reliability testing showed that the constant movement of the sample in and out of the chamber for room temperature testing resulted in swelling and shrinking of the adhesive causing a crack to initiate and propagate along the die-epoxy interface.

Acknowledgment

The author would like to acknowledge Enterprise Ireland CFTD /05 / 122 and HEA PRTLI-IV project NEMBES for providing the opportunity to carry out the work presented in this paper.

REFERENCES

[1] G. Bouma and W. Strober, "The immunological and genetic basis of inflammatory bowel disease", Nature Reviews Immunology, vol. 3, pp. 521-533, 2003.

[2] J. Lennard-Jones, "Classification of inflammatory bowel disease", Scandinavian Journal of Gastroenterology, vol. 24, pp. 2-6, 1989.

[3] R. Sartor, "Mechanisms of disease: pathogenesis of Crohn's disease and ulcerative colitis", Nature Clinical Practice Gastroenterology and Hepatology, vol. 3, p. 390, 2006.

[4] H. Battery, V. Capsule, E. Contract, and G. IDEAS, "Lab-on-a-Pill: The International Context of the Work: The invention of the transistor enabled".

[5] C. McCaffrey, O. Chevalerias, C. O'Mathuna, and K. Twomey, "Swallowable-capsule technology", IEEE Pervasive Computing, vol. 7, pp. 23-29, 2008.

[6] G. Costamagna, S. Shah, M. Riccioni, F. Foschia, M. Mutignani, V. Perri, A. Vecchioli, M. Brizi, A. Picciocchi, and P. Marano, "A prospective trial comparing small bowel radiographs and video capsule endoscopy for suspected small bowel disease", Gastroenterology, vol. 123, pp. 999-1005, 2002.

[7] K. Twomey and J. Marchesi, "Swallowable capsule technology: current perspectives and future directions", Endoscopy, vol. 41, pp. 357–362, 2009.

[8] "Philips Intellicap technology": http://www.research.philips.com/newscenter/backgrounders/081111-ipill.html.

[9] R. Allan, "Smart Pill Goes On A Fantastic Voyage", Electronic Design, vol. 54, pp. 27-66, 2006..

[10] R. Dettmer, "Fantastic voyage [wireless capsule endoscopes]", IEE Review, vol. 51, pp. 28-32, 2004.

[11] L. Wang, E. Johannessen, P. Hammond, L. Cui, S. Reid, J. Cooper, and D. Cumming, "A programmable microsystem using system-on-chip for real-time biotelemetry", IEEE Transactions on Biomedical Engineering, vol. 52, pp. 1251-1260, 2005.

[12] J. Cooper, E. Johannessen, and D. Cumming, "Bridging the gap between micro and nanotechnology: using lab-on-a-chip to enable nanosensors for genomics, proteomics, and diagnostic screening", Network and Parallel Computing, pp. 517-521, 2004.

[13] E. Johannessen, L. Wang, S. Reid, D. Cumming, and J. Cooper, "Implementation of radiotelemetry in a lab-in-a-pill format", Lab on a Chip, vol. 6, pp. 39-45, 2006.

[14] E. A. Johannessen, W. Lei, C. Li, T. Tong Boon, M. Ahmadian, A. Astaras, S. W. J. Reid, P. S. Yam, A. F. Murray, B. W. Flynn, S. P. Beaumont, D. R. S. Cumming, and J. M. Cooper, "Implementation of multichannel sensors for remote biomedical measurements in a microsystems format", Biomedical Engineering, IEEE Transactions on, vol. 51, pp. 525-535, 2004.

[15] T. Tang, E. Johannessen, L. Wang, A. Astaras, M. Ahmadian, L. Cui, A. Murray, J. Cooper, S. Beaumont, and B. Flynn, "IDEAS: a miniature lab-in-a-pill multisensor microsystem", 2002.

[16] R. Briegel, M. Ashauer, H. Ashauer, H. Sandmaier, and W. Lang, "Anisotropic conductive adhesion of microsensors applied in the instance of a low pressure sensor", Sensors and Actuators A: Physical, vol. 97-98, pp. 323-328, 2002.

[17] K. Saarinen and P. Heino, "Moisture effects on reliability of non-conductive adhesive attachments", in 2nd IEEE International Interdisciplinary Conference on Portable Information Devices, and the 7th IEEE Conference on Polymers and Adhesives in Microelectronics and Photonics, 2008, pp. 1-6.

[18] L. D. Burke and B. H. Lee, "An investigation of the electrocatalytic behaviour of gold in aqueous media", Journal of Electroanalytical Chemistry, vol. 330, pp. 637-661, 1992.

[19] E. Á. D. Eulate, "Investigation of an Electronic Tongue Array for Gastro-Intestinal Disease Detection", in Department of Chemistry, Master of Science Cork: University College Cork, 2007, unpublished.

[20] L. L. Mercado, J. White, V. Sarihan, and T. Y. T. Lee, "Failure mechanism study of anisotropic conductive film (ACF) packages", IEEE Transactions on Components and Packaging Technologies, vol. 26, pp. 509-516, 2003.

[21] J. F. J. M. Caers, X. J. Zhao, J. W. C. de Vries, E. H. Wong, G. Kums, and A. R. C. Engelfriet, "HART: A new highly accelerated robustness test for conductive adhesive interconnects", in 58th Electronic Components and Technology Conference, 2008, pp. 1695-1699.

[22] Y. Lin and J. Zhong, "A review of the influencing factors on anisotropic conductive adhesives joining technology in electrical applications", Journal of Materials Science, vol. 43, pp. 3072-3093, 2008.

[23] J. Liu, X.-z. Lu, and L.-q. Cao, "Reliability aspects of electronics packaging technology using anisotropic conductive adhesives", Journal of Shanghai University (English Edition), vol. 11, pp. 1-16, 2007.

[24] L. Teh, M. Teo, E. Anto, C. Wong, S. Mhaisalkar, P. Teo, and E. Wong, "Moisture-induced failures of adhesive flip chip interconnects", IEEE Transactions on Components and Packaging Technologies, vol. 28, pp. 506-516, 2005.

[25] C. Yin, H. Lu, C. Bailey, and Y. Chan, "Macro-micro modelling of moisture induced stresses in an ACF flip chip assembly", Soldering & Surface Mount Technology, vol. 18, pp. 27-32, 2006.

[26] C. Wu, J. Liu, and N. Yeung, "The effects of bump height on the reliability of ACF in flip-chip", Soldering & Surface Mount Technology, vol. 13, pp. 25-30, 2001.

[27] S. Gi-Dong, C. Chang-Kyu, P. Kyung-Wook, and L. Soon-Bok, "Experimental analysis on the mechanism of moisture induced interface weakening in ACF package", European Microelectronics and Packaging Conference, EMPC, pp. 1-7, 2009.

[28] G.-D. Sim, C.-K. Chung, K.-W. Paik, and S.-B. Lee, "Moisture induced interface weakening in ACF package", Materials Science and Engineering: A, vol. 528, pp. 698-705, 2010.

[29] T. Ferguson and J. Qu, "The Effect of Moisture on the Adhesion and Fracture of Interfaces in Microelectronic Packaging", in Micro- and Opto-Electronic Materials and Structures: Physics, Mechanics, Design, Reliability, Packaging, E. Suhir, Y. C. Lee, and C. P. Wong, Eds.: Springer US, 2007, pp. B431-B471.

[30] G. Xian and V. M. Karbhari, "DMTA based investigation of hygrothermal ageing of an epoxy system used in rehabilitation", Journal of Applied Polymer Science, vol. 104, pp. 1084-1094, 2007.